



Effect of Rapid-Mixing Duration on Floc Growth in the Coagulation of Peat Water with *Sesbania grandiflora* Seed as Measured by DinoCapture 2.0

Rudy Syah Putra^{1,2}(✉) and Farikhatul Fitria^{1,2}

¹ Department of Chemistry, Faculty of Mathematics and Natural Sciences, Universitas Islam Indonesia, Yogyakarta 55584, Indonesia

rudy.syahputra@uii.ac.id, 18612022@students.uii.ac.id

² Environmental Remediation Research Group, Department of Chemistry, Faculty of Mathematics and Natural Sciences, Universitas Islam Indonesia, Yogyakarta 55584, Indonesia

Abstract. The coagulation treatment was applied to the synthetic peat water using *Sesbania grandiflora* seed. One of the factors to enhance coagulation is rapid and slow mixing. Rapid mixing is crucial to promote the interaction of coagulant with suspended particles and the formation of micro flocs. While slow mixing is crucial to promote aggregation between microflocs. In this study, rapid mixing was varied from 5 to 10 and 15 min during the coagulation process. Microscopic method analysis was used to obtain the data using a camera and computer. Flocs formed are captured by DinoCapture 2.0 software equipped with a Dino-Lite handheld digital microscope resulting in microscopic images of the flocs. Afterward, direct measurement of a magnified floc image is applied by using a calibrated scale on the floc image, so a large number of floc sizes can be obtained. Image analysis results from DinoCapture 2.0 showed that the longer duration of the rapid-mixing time, the larger size of floc formed, but in contrast, the number of flocs decreased. The optimum time for rapid mixing was 5 min and 30 min for slow mixing, according to the highest number of flocs formed, with the floc size spread evenly under 0.2 mm. Rapid-mixing time of 5/30 min was applied to the coagulation of peat water so that the floc could grow well and coagulation could be carried out optimally. This is because a mixing time that is too short can reduce floc formation, but a very long mixing time can cause floc breakage.

Keywords: coagulation · DinoCapture 2.0 · floc · peat water rapid and slow-mixing · *Sesbania grandiflora* seed

1 Introduction

Coagulation is a water and wastewater treatment process that can reduce suspended particles [1]. In the treatment water facilities, coagulation processes are followed by flocculation and sedimentation [2]. The principle of coagulation is the destabilization of suspended particles by reducing the repulsive forces between the particles by adding

the coagulant. Destabilized particles then collide with each other to form a large size of floc which easily precipitates [3, 4]. The effectiveness of coagulation depends on several factors, for example, temperature, pH, coagulant type and dose, and mixing conditions. Mixing is a crucial process in coagulation. There are two types of mixing include rapid and slow mixing. Rapid mixing can promote the interaction of coagulants with suspended particles to form a micro floc, and slow mixing promotes the aggregation of micro floc to form a large floc or macro floc [5, 6]. A very short mixing time can decrease the rate of floc formation, whereas a considerably long mixing time can promote the breakdown of floc formation [7].

Many researchers found that both rapid and slow mixing conditions in the coagulation process significantly affect the size, strength, and structure of the floc. However, these properties are not easy to characterize due to the irregularity of the floc size and shape [8–11]. Various methods have been applied to characterize the floc properties (i.e., shape, size, and strength), such as light scattering, transmitted light using PDA 2000, and individual particle sensors [12]. Recently, microscopy observation has been applied to allow individual particles to be viewed, scrutinized, and analyzed at high magnification. This method allowed the researcher to get a feel for the structure of each floc under investigation and gave a better indication of floc shape and irregularity [12]. In addition, the method is relatively inexpensive compared to other methods. The combination of microscopy and image analysis software has been widely used to characterize the floc formation. A dino-Lite microscope can directly capture an object and measure the dimensions of the actual size of gas bubbles in the electroflotation process using image analysis, namely DinoCapture 2.0 software [13]. A video camera with an axioscop of Zeiss optical microscope has been applied for capturing the floc formation by ferric sulfate [14]. A digital imaging process with LabVIEW has been applied to measure the development of floc particles in the coagulation process [15]. Also, a coagulation process under the optimized conditions has been monitored by an in-situ microscope in conjunction with image analysis [16]. Those reports claimed that an easy-handle microscope with image processing analysis is important to study the development of floc formation during the coagulation process.

Therefore, in this study, a digital microscope is directly applied to observe floc formation during the coagulation by Turi (*Sesbania grandiflora*) in the treatment of peat water. Floc formation during the rapid and slow mixing process was captured by a Dino-Lite microscope, and then directly the image was measured by DinoCapture 2.0 software.

2 Materials and Methods

A. Preparation of Synthetic Peat Water

Synthetic peat water was treated by a coagulation process. A stock solution of 1000 mg/L of humic acid was prepared by dissolving 1 g of humic acid and 4 g of NaOH in 1 L of deionized water [17]. The solution was then filtered through a 0.45 μm of 47 mm membrane cellulose nitrate filter (Mdi Advanced Microdevices Pvt. Ltd, India) prior to storage in the darkroom at ambient temperature. The working solution of

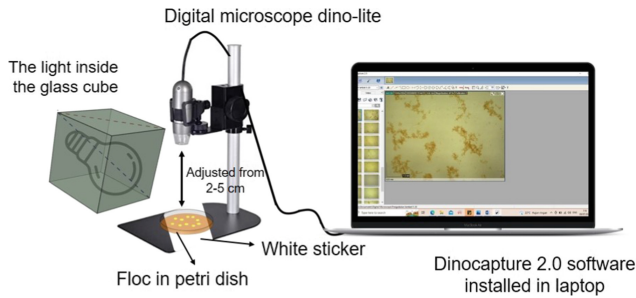


Fig. 1. Schematic diagram of capturing the floc image.

500 mg/L of humic acid was prepared by diluting a calculated amount of stock solution with deionized water. Also, metal-humic acid complexes are used in the coagulation experiments. Peat water with 100 mg/L iron (Fe) was prepared by diluting 0.05 g of $\text{Fe}(\text{NO}_3)_3 \cdot 9\text{H}_2\text{O}$ in a working solution. The pH 5 was then adjusted either by 0.1 M HCl or 0.1 M NaOH.

B. Effect of Time on Rapid and Slow Mixing in the Coagulation Process

Sesbania grandiflora of 1 g seed powder (i.e., 250 mesh/0.062 mm diameter) was added to synthetic peat water. The mixture was then rapid mixing (i.e., 5, 10, and 15 min) and continued with slow mixing for 30 min. The sample was then transferred into the Imhoff cone to precipitate for 24 h. The concentrated floc was put into a petri dish using a wide-mouthed pipette to prevent damaging the floc before dilution by 1:5 ratio to ensure an adequate particle distribution for microscopy observation [14]. These aqueous suspensions are preferred to prevent the flocs from falling on each other or agglomeration during the sample preparation. After the optimum rapid mixing time was obtained, the process was continued by varied slow mixing times (i.e. 15, 20, 25, and 30 min). The floc image was then captured by DinoCapture 2.0 software.

C. Floc Imaging and Analysis

The floc formation was captured by a digital microscope (AF4515-FIT Dino-Lite Edge, Anmo Electronics Corporation, Taiwan) with the resulting image resolution of 1280×1204 (1.3 Mp). The magnification was adjusted from 40–80 \times by the distance between the microscope (AF4515-FIT Dino-Lite Edge, Anmo Electronics Corporation, Taiwan), and the object was 2–5 cm. The microscope was connected to a notebook via USB 2.0 for image capture and focus adjustment. Captured image was calibrated by a scale in the calibration target sheet to obtain the actual floc size. Figure 1 shows a schematic diagram of capturing floc images with a digital microscope.

Table 1. Proximate Analysis of *Sesbania grandiflora* Seed

| Parameter (%) | | | | |
|---------------|-----|---------|-------|--------------|
| Water | Ash | Protein | Lipid | Carbohydrate |
| 9 | | | .6 | 53 |
| | | | 3.8 | |
| | | | 30.8 | |
| | | | 2.8 | |

3 Results and Discussion

A. Characterization of Turi (*Sesbania grandiflora*) as Natural Coagulant

Since chemical coagulants produce by-products that are harmful to the environment, the existence of alternative natural coagulants is used as an environmentally friendly technology [18]. However, natural coagulants have to contain proteins or polysaccharides with some functional groups that can promote adsorption, polymer bridging, and charge neutralization during the coagulation-flocculation process [1]. Table 1 shows the proximate analysis of the *Sesbania grandiflora* seed. In this regard, the seed had a protein content of as much as 30.8% and carbohydrate as much as 53%. In the coagulation-flocculation process, protein acts as polyelectrolytes that can release an opposite charge of a colloidal particle in water like a chemical [19]. Additionally, the polysaccharide is able to bind microflocs into larger aggregates with a faster deposition process due to the interaction between electrons π and OH- groups [20].

The 3276 cm^{-1} peak indicates the presence of O-H of the polysaccharide group [21], while the peak of 2923 cm^{-1} indicates a stretching of OH groups to the methyl group (C-OH). Wavenumber 1744 cm^{-1} indicates a C=O group of carboxylic acid, whereas 1536 cm^{-1} indicates an N-H of the protein group, and 1051 cm^{-1} indicates a C-O group [22] (Fig. 2).

The presence of OH, C=O, and C-O functional groups enabled the protein to be an efficient polyelectrolyte [23].

B. Effect of Mixing Time on the Flocculation-Coagulation Process

1) Measurement of floc size

Floc obtained was captured by digital microscope Dino-Lite, which was occupied with DinoCapture 2.0 software. As shown in Fig. 3, the floc particle has irregularity in shape (not circle nor spheric). However, according to the British standardized measurement, comparison between particles is only carried out if the particle is in the form of a circle or sphere shape. Based on that problem, Dharmarajah and Cleasby (1986) use the equivalent diameter in order to define the floc as a sphere or circle [12]. Furthermore,

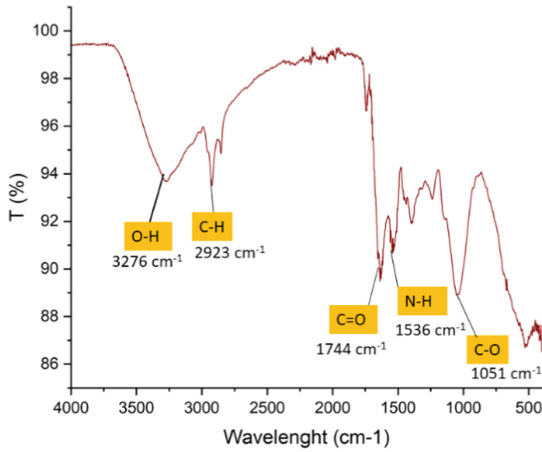


Fig. 2. FTIR spectra of *Sesbania grandiflora* seed.

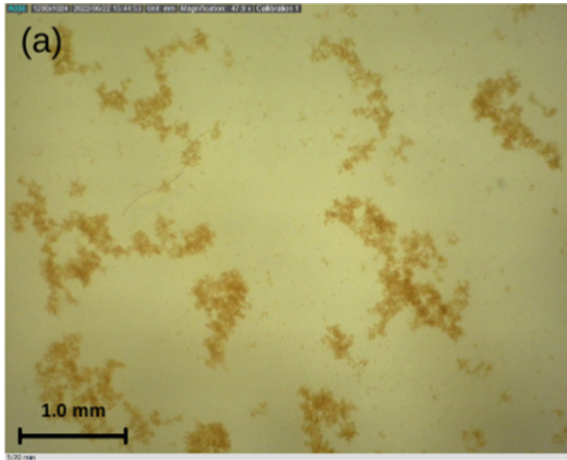


Fig. 3. The image of the floc captured by a digital microscope

when the term “floc size” is mentioned in many research, it refers to equivalent diameter. Therefore, in this study, floc size was served in equivalent diameter [24]. The equivalent diameter can be obtained from “Eq. 1” [24].

$$dec = \sqrt{\frac{4A_p}{\pi}} \quad (1)$$

Equation 1. Equivalent diameter formula

Where dec is the equivalent diameter (mm), A_p is the projected area (mm^2), and π is 3,14. The projected area can be obtained using the “lasso” tool that is prepackaged in Dino-Capture 2.0 software. As we trace, the projected area (mm^2) of the selection outline was obtained, as seen in Fig. 4.

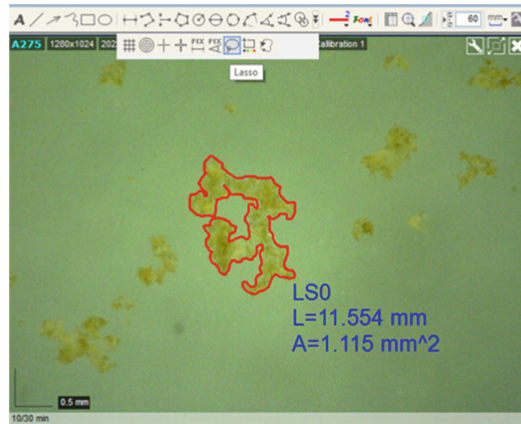


Fig. 4. Measurement of floc projected area using the “lasso” tool in DinoCapture 2.0 software

2) *Effect of mixing time on the floc size distribution*

Figure 5a, b, and c show the flocs formed during the rapid mixing times of 5, 10, and 15 min respectively. In general, flocs have an open structure with irregular branching. Flocs also have various conditions. Some of them have a single state, form clusters/groups with other flocs or form aggregations with other flocs. This finding was also presented in research conducted by [16]. Figure 5a shows the flocs formed at 5 min of rapid mixing. The flocs are denser and have a more closed structure compared to the other flocs (Figs. 5 b and c). In addition, there are small floc fragments around the larger floc. The floc fragments will agglomerate again, resulting in a high settling index and low turbidity. Based on the shape of the flocs produced, the floc formed during 5 min of rapid mixing follows a charge neutralization mechanism [25, 26]. Figure 5b shows the flocs formed at 10 min of rapid mixing. The flocs had a larger size (0.27 mm in average diameter) and a more open structure compared to the flocs formed at 5 min of rapid mixing. Figure 5c shows the flocs formed at 15 min of rapid mixing. Floc has the largest diameter (0.32 mm) and a more open structure because it has many branches. Floc like this is more difficult to break, but if it is broken, it will be irreversible. So that it cannot re-agglomerate with other flocs, and produces a low settling index, then increases the turbidity value [27]. It can be concluded that the longer the rapid mixing time, the larger the floc size and the decreased number of flocs. This happens because the floc formed during a short rapid mixing time will have a more closed shape which does not allow aggregation. Whereas at a longer rapid mixing time, the floc has a more open shape so that it can form aggregations with other flocs and produce larger flocs [9].

Figure 5d shows the size distribution of flocs at rapid mixing variation. The flocs formed in the Turi seed coagulation process were dominated by flocs with a diameter of <math><0.2\text{ mm}</math>. In more detail, during rapid mixing times of 5, 10, and 15 min the average floc diameter was 0.11 mm, 0.27 mm, and 0.32 mm, respectively, with the number of flocs being 1204, 795, and 507. As the mixing time increases, the floc diameter increases.

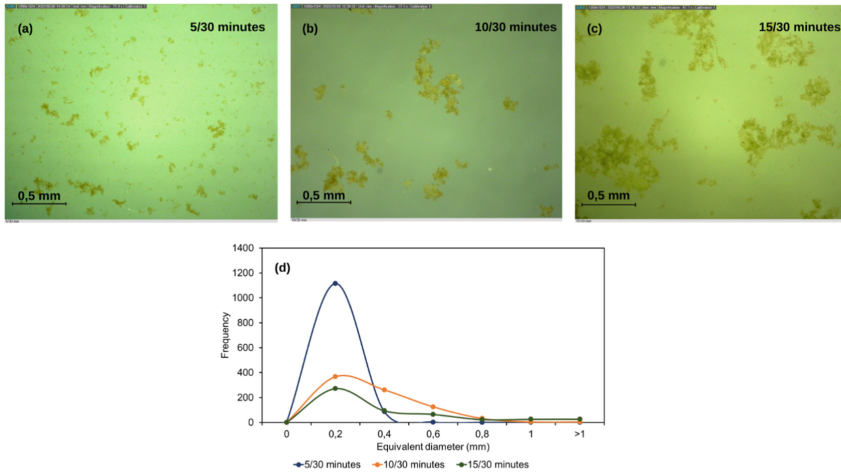


Fig. 5. Measurement of floc size using microscopy method under various rapid mixing times. Floc formed in 5 min (a), 10 min (b), 15 min of rapid mixing time (c), and distribution of floc size by different of rapid mixing time (d).

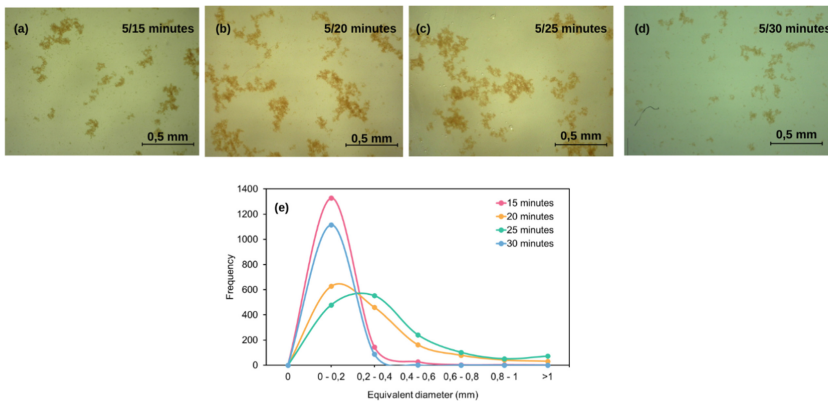


Fig. 6. Measurement of floc size using microscopy method under various slow mixing times. Floc formed in 15 min (a), 20 min (b), 25 min of slow mixing time (c), and distribution of floc size by different of slow mixing time (d).

However, the number of flocs decreased. This occurs because large flocs capture small flocs to form aggregates with larger diameters [16, 28].

Figure 6a, b, and c show the flocs formed during the slow mixing times of 15, 20, 25, and 30 min respectively. In general, flocs have an open structure with irregular branching. Flocs also have various conditions. Some of them have a single state, form clusters/groups with other flocs or form aggregations with other flocs. This finding was also presented in research conducted by [16]. Figure 6a shows the flocs formed at slow mixing for 15 min. It can be seen that the flocs are denser than the other flocs (Fig. 6 b and c). Floc also has a structure that is not very open because it only has a few branches.

In addition, there are fragments of small flocs around the large flocs. The floc fragments will agglomerate again, resulting in a high settling index and low turbidity [25, 26]. Based on the shape of the flocs obtained, the flocs formed at a slow mixing time of 15 min following the charge neutralization mechanism [25, 26]. Figure 6 b shows the flocs formed after 20 min of slow mixing. It can be seen that the floc has a larger diameter (0.31 mm on average) compared to the floc formed at 15 min of slow mixing (0.29 mm on average). In addition, the floc also has a more open shape because it has more branches. Figure 6c shows the flocs formed after 25 min of slow mixing. It can be seen that the floc has the largest diameter with an average size of 0.37 mm. In addition, flocs also have a more open shape because they have more branches.

Figure 6d shows the flocs formed after 30 min of slow mixing. A floc with a smaller diameter (0.11 mm) was produced compared to the floc formed at slow mixing for 25 min (0.37 mm). This occurs because the floc is broken due to the breaking of chemical bonds [27, 29]. In addition, the floc also becomes denser (high flocculation index). This finding was also presented by Peng and Williams [30], who stated that when the maximum floc diameter size has been reached, a decrease will follow it in floc diameter size [28]. In addition, it was also found that the small flocs formed would become denser with a higher flocculation index.

Figure 6 e shows the size distribution of the flocs formed at various slow mixing times. The flocs formed in the Turi seed coagulation process were dominated by flocs with a diameter of <0.2 mm. In more detail, the smallest floc diameter with an average size of 0.29 mm was found in 15 min of slow mixing with a total of 1509 flocs. Then the average floc diameter became larger with a size of 0.31 mm in 20 min of slow mixing with the total floc was 1497. The average diameter of the floc was the largest, with a size of 0.37 mm at a slow mixing time of 25 min with a total floc of 1400. As the slow mixing time increased, the floc diameter increased. However, the number of flocs decreased. This occurs because large-diameter flocs capture small-diameter flocs to form aggregates with larger diameters [16, 19]. However, the average floc diameter then decreased to 0.11 mm at slow mixing for 30 min with a total of 1204 flocs because large flocs broke due to the breaking of chemical bonds [27, 29]. Based on the floc size distribution, the optimum slow mixing time is 30 min. This finding is in accordance with other studies that found that the optimal duration of slow stirring is not only the time to form the largest average floc size but longer because larger flocs have smaller fractional dimensions and therefore settling index is low [31–33].

It can be concluded that the mixing time is directly proportional to the size of the floc diameter. However, it is inversely proportional to the number of flocs. As the mixing time increases, the average diameter of the flocs increases, and the number of flocs decreases. During rapid mixing times of 5, 10, and 15 min, the average floc diameter was 0.11 mm, 0.27 mm, and 0.32 mm, respectively, with the number of flocs being 1204, 795, and 507, respectively. At the slow mixing times of 15, 20, 25, and 30 min, the average diameter size of flocs was 0.29 mm, 0.31 mm, 0.37 mm, and 0.11 mm, respectively, with the number of flocs being 1509, 1497, 1400, 1204. As the mixing time increases, the size of the floc diameter increases. However, the number of flocs decreased. This occurs because small-diameter flocs are captured by large-diameter flocs to form aggregates with larger diameters [16, 19].

4 Conclusion

The microscopy method evaluated the effect of mixing time, both rapid and slow mixing. In this study, the microscopy method was carried out by counting the size and the total of floc using a digital microscope, namely Dino-Lite, which specifically uses the lasso tool prepackaged from the Dino-Lite manufacturer. Then, the floc size distribution was produced to monitor the effect of mixing time. The result shows that 5 min is the optimum time for rapid mixing, and 30 min is the optimum time for slow mixing.

Acknowledgement. The authors acknowledge grants from Universitas Islam Indonesia through Collaborative Research (contract no. 3686/Rek/10/DSDM/XI/2020).

References

1. Kurniawan SB, Imron MF, Chik CENCE, et al (2022) What compound inside biocoagulants/biofloculants is contributing the most to the coagulation and flocculation processes? *Sci. Total Environ.* 806
2. Muruganandam L, Kumar S, Jena A, et al (2017) Treatment of waste water by coagulation and flocculation using biomaterials. *IOP Conf Ser Mater Sci Eng* 263:032006. <https://doi.org/10.1088/1757-899X/263/3/032006>
3. Aktas TS, Fujibayashi M, Maruo C, et al (2013) Influence of velocity gradient and rapid mixing time on flocs formed by polysilica iron (PSI) and polyaluminum chloride (PACl). *Desalin Water Treat* 51:4729–4735. <https://doi.org/10.1080/19443994.2012.751883>
4. Fard MB, Hamidi D, Yetilmezsoy K, et al (2021) Utilization of Alyssum mucilage as a natural coagulant in oily-saline wastewater treatment. *J Water Process Eng* 40: <https://doi.org/10.1016/j.jwpe.2020.101763>
5. Duan J, Gregory J (2003) Coagulation by hydrolysing metal salts. *Adv Colloid Interface Sci* 100–102:475–502. [https://doi.org/10.1016/S0001-8686\(02\)00067-2](https://doi.org/10.1016/S0001-8686(02)00067-2)
6. BinAhmed S, Ayoub G, Al-Hindi M, Azizi F (2015) The effect of fast mixing conditions on the coagulation–flocculation process of highly turbid suspensions using liquid bittern coagulant. *Desalin Water Treat* 53:3388–3396. <https://doi.org/10.1080/19443994.2014.933043>
7. Kurniawan SB, Abdullah SRS, Imron MF, et al (2020) Challenges and opportunities of biocoagulant/biofloculant application for drinking water and wastewater treatment and its potential for sludge recovery. *Int. J. Environ. Res. Public Health* 17:1–33
8. Gregory J, Dupont V (2001) Properties of flocs produced by water treatment coagulants. *Water Sci Technol* 44:231–236. <https://doi.org/10.2166/WST.2001.0628>
9. Yukselen MA, Gregory J (2004) The reversibility of floc breakage. *Int J Miner Process* 73:251–259. [https://doi.org/10.1016/S0301-7516\(03\)00077-2](https://doi.org/10.1016/S0301-7516(03)00077-2)
10. Jarvis P, Jefferson B, Gregory J, Parsons SA (2005a) A review of floc strength and breakage. *Water Res.* 39:3121–3137
11. Jarvis P, Jefferson B, Parsons SA (2006) Floc structural characteristics using conventional coagulation for a high doc, low alkalinity surface water source. *Water Res* 40:2727–2737. <https://doi.org/10.1016/j.watres.2006.04.024>
12. Jarvis P, Jefferson B, Parsons SA (2005c) MEASURING FLOC STRUCTURAL CHARACTERISTICS. *Rev Environ Sci Biotechnol* 4: 1–18

13. Putra RS, Arrunillah D, Fitria F, Ripki N (2021) Measurement of Gas Bubbles Distribution on Electroflotation Process Using Titanium and Stainless Steel Electrode with DinoCapture 2.0. In: *HeNce 2021-2021 IEEE Int Conf Heal Instrum Meas Nat Sci*. <https://doi.org/10.1109/InHeNce52833.2021.9537227>
14. Aguilar MI, Saez JS, Llorens M, et al (2003) Microscopic observation of particle reduction in slaughterhouse wastewater by coagulation-flocculation using ferric sulphate as coagulant and different coagulant aids. *Water Res* 37:2233–2241
15. Sun S, Weber-Shirk M, Lion LW (2016) Characterization of Flocs and Floc Size Distributions Using Image Analysis. *Environ. Eng. Sci.* 33:25–34
16. Nunes GS, Sammarro Silva KJ, Souza Freitas BL, et al (2022) In-situ microscopy investigation of floc development during coagulation-flocculation with chemical and natural coagulants. *Sep Sci Technol* 00:1–11. <https://doi.org/10.1080/01496395.2022.2056055>
17. Sudoh R, Islam MS, Sazawa K, et al (2015) Removal of dissolved humic acid from water by coagulation method using polyaluminum chloride (PAC) with calcium carbonate as neutralizer and coagulant aid. *J Environ Chem Eng* 3:770–774. <https://doi.org/10.1016/j.jece.2015.04.007>
18. Ang WL, Mohammad AW, Benamor A, Hilal N (2016) Chitosan as natural coagulant in hybrid coagulation-nanofiltration membrane process for water treatment. *J Environ Chem Eng* 4:4857–4862. <https://doi.org/10.1016/J.JECE.2016.03.029>
19. Hoong HNJ, Ismail N (2018) Removal of Dye in Wastewater by Adsorption-Coagulation Combined System with Hibiscus sabdariffa as the Coagulant. In: *MATEC Web of Conferences*. EDP Sciences
20. Maćczak P, Kaczmarek H, Ziegler-Borowska M (2020) Recent Achievements in Polymer Bio-Based Flocculants for Water Treatment. *Materials (Basel)* 13. <https://doi.org/10.3390/MA13183951>
21. Pavan FA, Lima EC, Dias SLP, Mazzocato AC (2008) Methylene blue biosorption from aqueous solutions by yellow passion fruit waste. *J Hazard Mater* 150:703–712. <https://doi.org/10.1016/J.JHAZMAT.2007.05.023>
22. Gottipati R, Mishra S (2010) Application of biowaste (waste generated in biodiesel plant) as an adsorbent for the removal of hazardous dye - methylene blue - from aqueous phase. *Brazilian J Chem Eng* 27:357–367. <https://doi.org/10.1590/S0104-66322010000200014>
23. Amran AH, Zaidi NS, Syafiuddin A, et al (2021) Potential of Carica papaya Seed-Derived Bio-Coagulant to Remove Turbidity from Polluted Water Assessed through Experimental and Modeling-Based Study. *Appl Sci* 2021, Vol 11, Page 5715 11:5715. <https://doi.org/10.3390/APP11125715>
24. Cousin CP, Ganczarczyk JJ (1998) Effects of salinity on physical characteristics of activated sludge flocs. *Water Qual Res J Canada* 33:565–587. <https://doi.org/10.2166/WQRJ.1998.032>
25. Tan BH, Ravi P, Tan LN, Tam KC (2007) Synthesis and aqueous solution properties of sterically stabilized pH-responsive polyampholyte microgels. *J Colloid Interface Sci* 309:453–463
26. Lee CS, Robinson J, Chong MF (2014) A review on application of flocculants in wastewater treatment. *Process Saf Environ Prot* 92:489–508. <https://doi.org/10.1016/j.psep.2014.04.010>
27. Yu W, Li G, Xu Y, Yang X (2009) Breakage and re-growth of flocs formed by alum and PACl. *Powder Technol* 189:439–443. <https://doi.org/10.1016/j.powtec.2008.07.008>
28. Bouyer D, Line A, Cockx A, Do-Quang Z (2001) Experimental analysis of floc size distribution and hydrodynamics in a jar-test. *Chem Eng Res Des* 79:1017–1024. <https://doi.org/10.1205/02638760152721587>

29. 30. Ayoub GM, BinAhmed SW, Al-Hindi M, Azizi F (2014) Coagulation of highly turbid suspensions using magnesium hydroxide: Effects of slow mixing conditions. *Environ Sci Pollut Res* 21:10502–10513. <https://doi.org/10.1007/s11356-014-2857-0>
30. 31. Peng, S. J., & Williams, R. A. (1994). Direct measurement of floc breakage in flowing suspensions. *Journal of colloid and interface science*, 166(2), 321-332.
31. 32. Johnson CP, Li X, Logan BE (1996) Settling Velocities of Fractal Aggregates. *Environ Sci Technol* 30:1911–1918. <https://doi.org/10.1021/es950604g>
32. Gregory J (1997) The density of particle aggregates. *Water Sci Technol* 36:1–13. [https://doi.org/10.1016/S0273-1223\(97\)00452-6](https://doi.org/10.1016/S0273-1223(97)00452-6)
33. Gregory J (1998) The role of floc density in solid-liquid separation. *Filtr Sep* 35:366–367. [https://doi.org/10.1016/S0015-1882\(97\)87417-4](https://doi.org/10.1016/S0015-1882(97)87417-4)

Open Access This chapter is licensed under the terms of the Creative Commons Attribution-NonCommercial 4.0 International License (<http://creativecommons.org/licenses/by-nc/4.0/>), which permits any noncommercial use, sharing, adaptation, distribution and reproduction in any medium or format, as long as you give appropriate credit to the original author(s) and the source, provide a link to the Creative Commons license and indicate if changes were made.

The images or other third party material in this chapter are included in the chapter's Creative Commons license, unless indicated otherwise in a credit line to the material. If material is not included in the chapter's Creative Commons license and your intended use is not permitted by statutory regulation or exceeds the permitted use, you will need to obtain permission directly from the copyright holder.

